PERGAMON International Journal of Impact Engineering 26 (2001) 797–808

INTERNATIONAL JOURNAL OF IMPACT ENGINEERING

www.elsevier.com/locate/ijimpeng

ANALYSIS AND TESTING OF ROD-LIKE PENETRATORS IN THE 4-5 KM/S VELOCITY REGIME[1]

JOHN VETROVEC*, REES PADFIELD*, DANIEL SCHWAB*, PETER NEBOLSINE**, RICHARD HAYAMI***, MARK ZWIENER***, JOHN HUNTINGTON****, and STEVEN L. HANCOCK****

*Rocketdyne Propusion & Power, The Boeing Company, 6633 Canoga Avenue, Canoga Park, Calif. 91309, U.S.A.; **Physical Sciences Inc. (PSI), Andover, MA, U.S.A.; ***University Of Alabama in Hunstville (UAH), Hunstville AL, U.S.A.; ***Huntington Research and Engineering (HRE), San Jose, CA, U.S.A

Abstract — This work describes the analysis and ballistic range testing to evaluate the performance of rod-like Kill Enhancement Device (KED) penetrators on of multi-layered targets covering large range of densities including high-density material. Tests showed that (1) high-density material can be penetrated at oblique angles of incidence without projectile fragmentation and (2) high explosive within the target can be initiated. Test data from experiments was compared to predictive analyses generated by hydrocodes and found to be in excellent agreement.

Keywords: kill enhancement device, rod penetrators, high-explosive initiation, ballistic testing

INTRODUCTION AND SUMMARY

The lethality of hit-to-kill interceptors is sensitive to its hit point relative to the target payload. Uncertainty in the aimpoint combined with inherent kill vehicle (KV) maneuvering system errors reduce the likelihood of the KV impacting the vulnerable area of the target. Potentially, an intercept with glancing body-to-body collision could only damage the heatshield and aeroshell while leaving an intact weapon in a "crippled" delivery vehicle. Studies conducted by the U.S. Government, Boeing, and others have shown that the detrimental effect of aimpoint selection and maneuvering error on lethality can be ameliorated by a kill enhancement device (KED) using an array of rod-like penetrators that protrudes beyond the KV body envelope. Recent work done by Boeing shows that a KED penetrator array can greatly increase the lethal footprint of the KV while adding only small increases to weight and cost.

The effort described in this paper was conducted to study hypervelocity impact of rod-like, tungsten alloy projectiles into complex multi-layered targets with large range of densities. Key element of this work was ballistic range testing at impact velocities near 5 km/s conducted at both normal impact and oblique impact. In addition to measurements of penetration depth and residual penetrator length at selected locations, the initiation of high explosive (HE) deep within the plate array target was demonstrated. Test data from each experiment was compared to predictive analyses generated by 2-D CALE and 3-D CTH hydrocodes and found to be in an excellent agreement in all evaluated areas: projectile erosion rates, penetration through high-density material at oblique incidence, and initiation of high explosive. This agreement provides confidence for the use of hydrocodes to investigate rod performance in velocity regimes not

[1]) The US Army Space and Missile Defense Command (SMDC), Huntsville, AL supported this effort under the Ground Based Interceptor (GBI) contract to The Boeing Company; Contract No. DASG60-90-C-0165.

0734-743X/01/$ - see front matter
PII: S0734-743X(01)00133-6

accessible on a ballistic range. Test data also provided an anchor for a fast running semi-empirical systems engineering model for projectile erosion and penetration.

BACKGROUND

The penetration performance of rod projectiles has been extensively investigated, often below ~3 km/s. Zukas [1] explains general impact physics and provides experimental examples for a variety of projectiles, impact parameters and target geometries. Anderson et al. [2] is a compendium of rod impact data from a number of investigators for impacts into semi-infinite targets and finite thickness plates. For higher impact velocities, Baker [3] and Baker and Williams [4] describe a single large data base for a variety of projectile and target plate materials principally in the 4 to 6 km/s range. Nebosine *et al.* [5] is a statistical analysis of that data base. Most of the published data is for either semi-infinite targets or single plate targets. A relatively small fraction of published work for rod impacts is for complex targets made up of layers of materials with varying densities (including high density, e.g., ~17 g/cm^3), thickness, porosities, etc. which is the case for this paper. Hohleer and Stilp [6] is one of the rare examples of rod impact data of tungsten alloy rods into tungsten alloy (in this case a semi-infinite target). Of the large data base presented in [3] only a few tests were performed for high density rod and plate materials at ~3 km/s. Absence of suitable data for anchoring computer simulations, particularly in the higher velocity regime and for complex targets makes computer simulation results open to question.

Another area of concern was integrity of the rod projectile after impacting high-density material at oblique angles of incidence. Fragmentation of rod projectiles made of brittle materials under such conditions has been observed at low impact velocities (below ~2 km/s) [1]. (The issue was remedied with the use of tougher projectile materials.) Projectiles with length /diameter ~ 1 are know to fragment when impacting plates even at normal incidence. Nebolsine *et al.* [7] is an example for tungsten alloy pellets impacting aluminum plates while [8] addresses theory and data for a tungsten alloy pellet impacting pure tungsten plates at 6.7 km/s and also aluminum plates. In addition to fragmentation, at relatively high impact velocities, some of the tungsten projectile and target plate material will remain molten after shock wave relief. At impact velocities higher than the speed of sound in the rod material, the impact shock propagates through the rod slower than the rod velocity. When penetrating through dense material, the rod erosion boundary actually moves faster than the shock from the initial contact. All of this suggests that, under these conditions, rod made of tough material is unlikely to fragment, at least at normal incidence. However, at oblique angles of incidence, asymmetric forces acting on the rod may cause it to shear into fragments.

In some applications, KED's may be used against reactive targets and may be specifically designed to initiate HE within the target. A key factor in causing HE initiation (HEI) is the impact-generated pressure, which is primarily affected by the projectile velocity. Normally, hydrocode simulations can provide reliable predictions of pressures generated by KED rod projectiles. However, the physics becomes more involved when penetrating through a complex, layered target, whose quantitative description may not be completely known. Boeing has been developing KED's for many years. During that period a fast running shotline processing code REAPER was developed for Boeing by PSI. REAPER, which is based on Baker's model [3,4], can process thousands of shotlines per minute, which makes it a highly suitable tool for system level KED lethality studies. Also, KED rod material was optimized for several applications by Nebolsine and Lo [9]. Obtaining data on rod performance in the higher velocity regime was deemed essential for reliable assessment of KED performance.

EXPERIMENTAL WORK

Test Preparations

Test Facility. The experimental part of the project was carried out at the ballistic range of the UAH ARC located at the U.S. Army Redstone Arsenal, Huntsville, AL. The light gas gun (LGG) system (schematically shown in Figure 1 and in photographs in Figure 2) used to perform the tests comprised of a 133-mm-diameter pump tube and a 28.8-mm launcher.

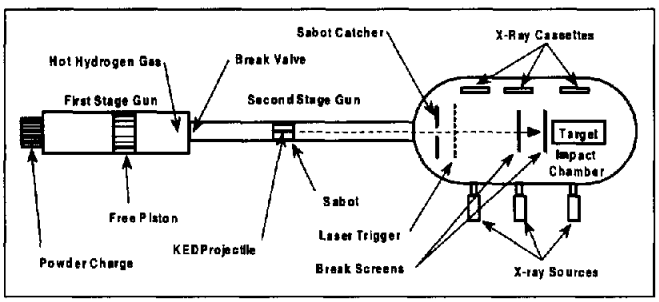

Figure 1. LGG launcher system schematic

In an LGG, a powder charge is used to drive a free piston to compress and adiabatically heat a reservoir of hydrogen gas. A break valve is opened when maximum energy has been deposited into the gas and hot gas is expanded in the launch tube where it accelerates a sabot-mounted projectile to velocities of several km/s. After leaving the launch tube, the sabot is separated from the projectile and is stopped by the sabot catcher. The projectile passes through laser trigger zone, break screens and impacts the target.

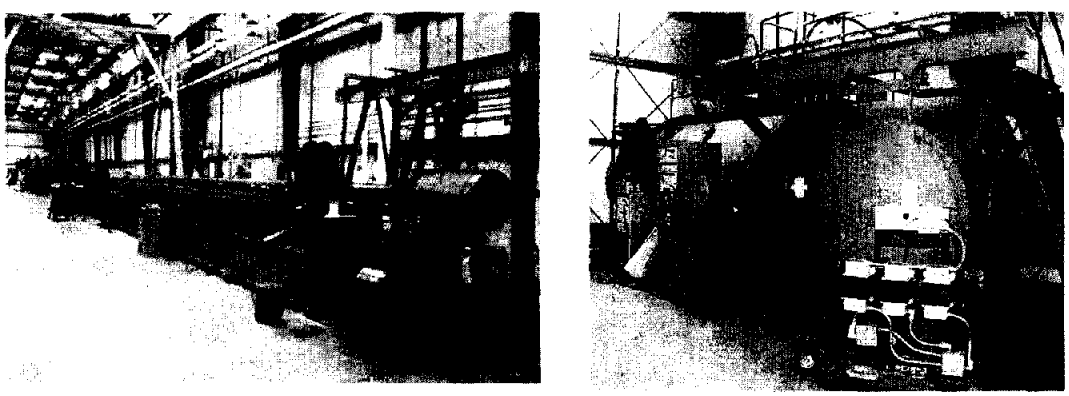

Figure 2. 133-mm LGG launcher system: left- a view down-range, right- impact chamber

Instrumentation and Diagnostics. LGG instrumentation comprised of flash x-rays, break screens, laser trigger, and cap pins. Three x-ray stations were used: the flight and pre-impact stations to verify projectile pitch and yaw prior to target penetration, and the impact station to capture the projectile image within the target. Each station used two x-ray sources mounted on the exterior of the target chamber and directing beams in mutually orthogonal directions, Figure 3. X-ray film cassettes were located inside the chamber and protected against shrapnel by sheets of plywood, Figure 4.

The pre-impact x-rays were triggered by interruption of a laser beam and captured the images of the projectile passing though the break screen 1. Break screen 2 attached to the target surface and centered on the planned shotline was used to trigger the impact zone x-ray after a preset time delay. Projectile velocity was first inferred from the time of flight measured by the two break

screens and corrected using x-ray images from flight and pre-impact stations. Typical images from the x-rays at the pre-impact and impact stations are shown in Figure 5. Pre-impact images were also used to determine projectile pitch and yaw. Projectile angle of attack at impact was calculated as the root-sum-square of the yaw and pitch angles measured on the pre-impact x-rays. Images of the impact x-rays revealed the residual projectile integrity, length, and angle of attack.

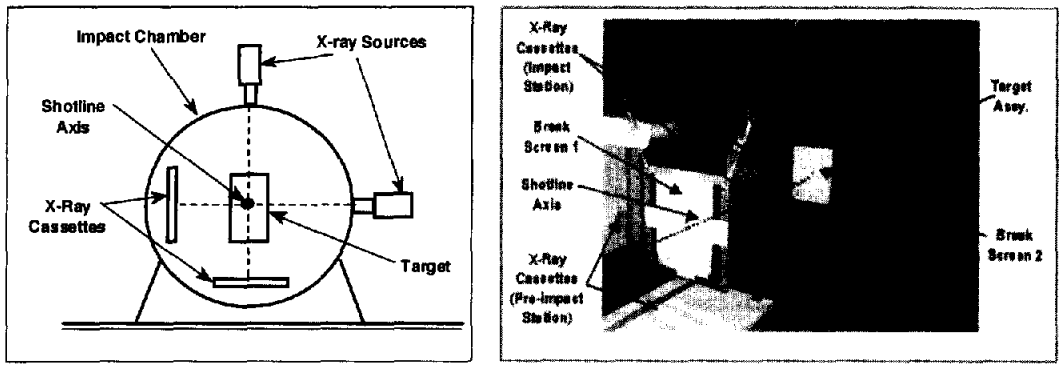

Figure 3. Typical x-ray station

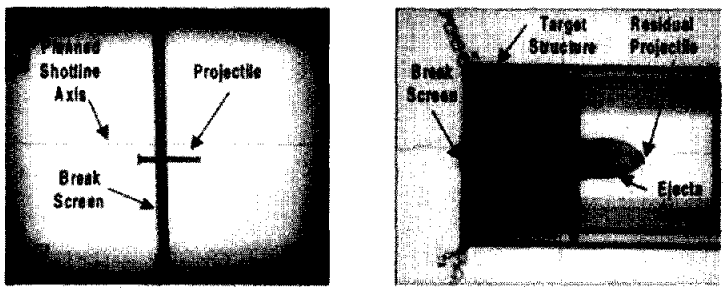

Figure 5. Typical images from x-rays at pre-impact (left) and impact (right) stations

KED Rod Projectiles. All test rods were made of a tungsten alloy that has been previously identified to possess superior toughness and resistance to impact fragmentation [9]. The rod diameter was chosen for convenience to be the large diameter of the 10-32 UNF machine thread, or 0.1865 inch. Threading of the rods was intended to provide sufficient engagement area to transfer launch loads to the sabot. Rods of two lengths were tested: 58 mm and 85 mm.

During launch, the projectile was held in a sabot shown in Figure 6. The core of the sabot, which engages threaded surface of the projectile was made of aluminum to withstand the contact pressures generated by the launch acceleration. To save weight, the remaining part of the sabot was made of nylon. The sabot was azimuthally split into four identical sections engaged together by a spline. After leaving the launch tube, aerodynamic forces separated the sabot sections from the projectile. Proper sabot design was critical to achieving uniform separation of sabot segments without impressing an excessive angle of attack onto the projectile. A conical tail fin made of titanium alloy was screwed to the aft section of the projectile to provide increased base area to support the launch stresses and to aero-stabilize the projectile prior to target impact.

Test Targets. Test targets were configured as stacks of plates and filler material with projected frontal area of approximately 6 by 10 inches. Various combinations of materials and thickness were used to study specific cases of interest. Targets were constructed from commercially available materials and stock thickness. Excluding the first two "development" shots that used simple targets, three types of complex targets were used. In the Type 1 target all the plates were positioned at normal incidence. In the Type 2 target all the plates were also

positioned at normal incidence but the thickness of the plates and stack were increased. In the Type 3 target selected plates were positioned at an incidence angle of approximately 45 degrees.

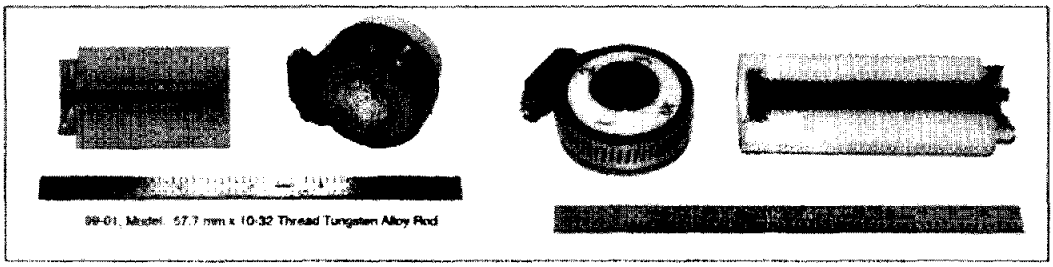

Figure 6. View of the sabot with the 58-mm rod (left) and 85-mm rod (right)

At two instances targets were modified to introduce a gap between adjacent plates that would permit clear x-ray of the residual projectile after partial target penetration. A layer of HE was incorporated into two of the Type 3 targets. Each (primary) target was provided with a secondary target consisting of six parallel mild steel plates 0.25 inch thick and separated by about 2 inches. The purpose of the secondary target was to dissipate energy of a projectile that may pass through the primary target. Target assemblies consisting of the primary and secondary targets suspended in the impact chamber on chains are shown in Figure 7. All test targets were fabricated at UAH ARC machine shop.

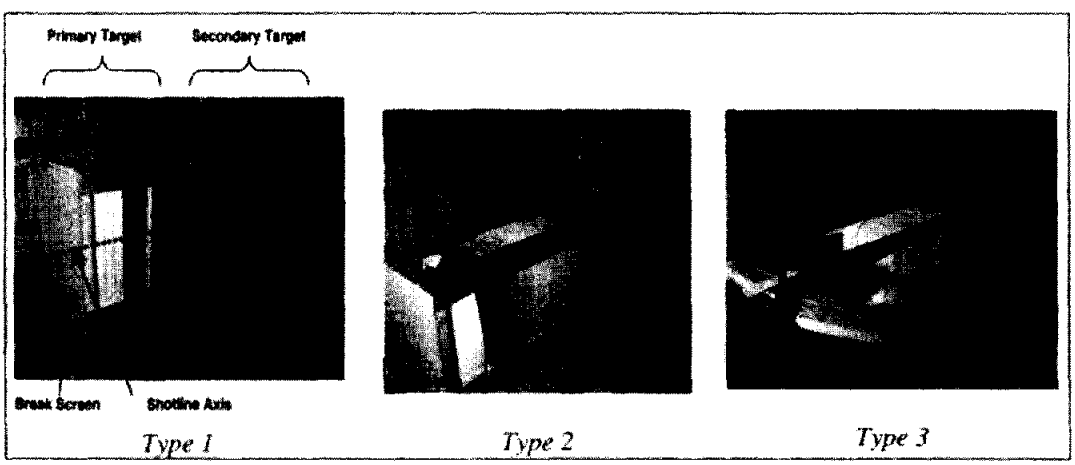

Figure 7. Target assembly showing the primary and secondary targets

Tests for evaluation of HEI were conducted on Type 3 targets. To accommodate HE, a circular cavity was machined into a PVC plate and filled with a puck of HE. To allow distinguishing between HEI types (explosion vs. conflagration), targets containing HE were instrumented with cap (aka shorting) pins located in proximity of the HE. Cap pins operate as pressure switches and are frequently used to obtain the time of shock wave arrival. Velocity of the shock wave can be inferred from the time-of-arrival (TOA) data. TOA sensed by the cap pins was used to calculate the shock wave velocity between adjacent pins. Velocity of the shock would be an indicator of HE burn mode: detonation (>> 1 km/s) or deflagration (<1 km/s). To avoid damage to x-ray sources, cassettes, and other instrumentation from HE blast and shrapnel, targets containing HE were placed inside a large diameter steel pipe, Figure 8. The pipe had two circular openings (about 6 inches in diameter) to allow x-ray exposure of the residual projectile just upstream of the HE puck. Additional protection of the x-ray sources and cassettes was provided by two sheets of plywood covering each of the 6-inch openings. Finally, the pipe ends

were covered by flat rectangular blast shields hung on rails. The forward blast shield had an opening for the projectile.

Launch Conditions. LGG launch velocity is intrinsically limited to just over 7 km/s but the practical limit is influenced by the mass of the projectile-sabot assembly. Figure 9 shows previous high-velocity launch data from the 133-mm LGG used in this project. To avoid the risk of launch failure, it was decided to conduct testing at velocities near 5 km/s. The actual launch velocities attained in the tests ranged from 4.38 to 4.87 km/s. Another important launch parameter is the projectile angle of attack, which must be limited to prevent the aft end of the projectile from striking the edges of the crater produced by the leading end.

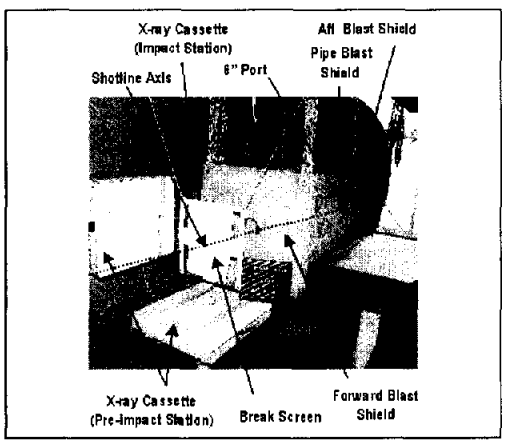

Figure 8. Target installation for tests with high explosive

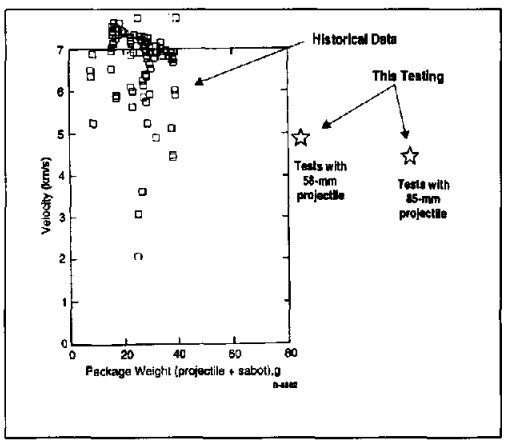

Figure 9. High-velocity launch data from the 133 mm LGG at UAH

Summary of Test Results

Test Matrix. Nine ballistic tests were conducted. The first two tests were development tests (shots) intended to validate the test setup, sabot design, and launch parameters. The following seven tests were "data shots." All data shots were conducted with complex, multi-layered targets. As planned, testing addressed all the KED rod issues, namely rod erosion at high velocities, rod shatter (especially when impacting at oblique incidence), and HEI. Table 1 is a test matrix summarizing test conditions, key results, and a correlation between tests and the KED rod issues.

Development Tests. Development shots were conducted against simple targets comprising of a composite plate and a secondary target (projectile catcher) in the test 99-46, and a composite plate, tungsten alloy plate, and a secondary target in the test 99-48. In the first development shot (99-46), the timing on the x-ray trigger was not set correctly and images of the rod in flight were not captured. The projectile penetrated the composite material and six plates of the secondary target. In the second (and last) development shot (98-48), the projectile was launched with a very small (2.5 degrees) angle of attack, thereby verifying launch conditions and the sabot design. The x-ray timing problem was corrected and images of residual projectile were captured downstream of the tungsten plate. The projectile also penetrated five plates of the secondary target.

57-mm Rod Tests. Both 58-mm rod tests were conducted on Type 1 target. In the 98-51 shot, the projectile penetrated the target as predicted, although its angle of attack exceeded the desirable limit. In the 99-01 test, a 6-inch gap was introduced in the target after the aluminum plate holding the high density material plate, and an unobstructed x-ray image of the residual projectile was captured, Figure 10-e.

Table 1. Test matrix summarizing test conditions and results

Test			Projectile			Target				KED Rod Issue Addressed		
No.	UAH No.	Date	Length [mm]	Velocity [km/s]	Attack < [deg]	Type	Angle of Incidence	HE	Notes	Erosion	Shatter	HEI
1	98-46	10-06-98	58	<5 est	NA	NA	Normal	No	Composite + secondary target only	√		
2	98-48	10-20-98	58	4.87	2.5	NA	Normal	No	Composite + high density plate + secondary target only	√		
3	98-51	10-29-98	58	4.75	11.9	1	Normal	No	All plates at ⊥ incidence	√		
4	99-01	01-13-99	58	4.83	2.2	1	Normal	No	All plates at ⊥ incidence, 6" gap down-stream of high density plate	√		
5	99-02	01-26-99	85	4.46	1.0	2	Normal	No	All plates at ⊥ incidence	√		
6	99-03	02-08-99	85	4.38	0.2	3	Oblique	No	Some plates at ∠ incidence	√	√	
7	99-04	03-26-99	85	4.47	1.9	3	Oblique	No	Some plates at ∠ incidence, 6" gap	√	√	
8	99-08	05-25-99	85	4.38	13.7	3	Oblique	YES	Some plates at ∠ incidence	√	√	√
9	99-09	05-27-99	85	4.44	1.8	3	Oblique	YES	Some plates at ∠ incidence	√	√	√

85-mm Rod Tests. The first 85-mm rod test (99-02) was conducted on a Type 2 target. The test verified the sabot design, launch capability, and penetration performance of the 85-mm long rod. Radiograph of the rod inside the target is not very clear and allowed only a rough assessment of residual rod length (~27 mm). The following tests were conducted on Type 3 targets. The 99-03 test x-ray images showed a cluster of large fragments obscuring the residual projectile after passing through the tungsten plate. To obtain a clearer view of the projectile in the following 99-04 test, a 6-inch gap was introduced downstream of the tungsten plate. Radiographs of the residual rod material were much clearer than in the preceding test and showed apparent rotation of the projectile, Figure 14. This was subsequently confirmed by 3-D CTH hydrocode simulation. CALE and CTH hydrocode simulations predicted that the combined penetrating power of the projectile material was sufficient to initiate the HE. This was later verified in the HEI tests.

HEI Tests. The two HEI tests (99-08 and 99-09) had the same target geometry and launch conditions as the 99-03 test. In both cases, the HE puck inside the target was initiated. In the 99-08 test, the projectile was launched with a significant angle of attack (13.7 degrees), but this did not impede successful HEI. In the 99-09 test, x-ray image of the projectile just upstream of the HE layer was obtained.

Comparing reconstructed projectile timeline with cap pin data strongly suggest that detonation (rather than deflagration) mode of burn took place in each test. Such information was deduced from timeline of events. For example, in the 99-09 test the average velocity of the initial radially expanding shock wave (in the HE and PVC) was estimated at 6.11 km/s, which is a clear evidence of a detonation (rather than deflagration).

COMPARISON OF TEST RESULTS AND COMPUTER SIMULATIONS

Test data generated in this project was compared to predictive analyses generated by 2-D CALE hydrocode under license from the Lawrence Livermore National Laboratory and a 3-D CTH hydrocode under license from the Sandia National Laboratory. Table 2 shows that there is an excellent correlation between residual rod length test data and hydrocode simulations. Such a closure between test data and CALE/CTH hydrocode simulations provides confidence in using the hydrocode for investigation of KED rod lethality in velocity regimes that are not accessible at ballistic ranges. The test data also provided a unique opportunity to verify the CALE hydrocode and to anchor the REAPER model.

Table 2. Correlation between tests and applicable predictive analyses

Test	Projectile Angle of Attack [deg]	Length of Residual Rod Impacting HE [mm]	
		Test Data (x-rays)	2-D Hydrocode
98-48	2.5	30	
98-51	11.9	No data	14
99-01	3.2	14	14
99-02	2.9	~27	~25
99-03	0.2	13	13
99-04	1.9	10	13
99-08	13.7	No data	13
99-09	1.8	12	13

Figure 10 shows an example of how computer simulations were compared to test data. Figure 10-c,d are respectively an enlargement of the simulation frame at the time of x-ray (48 μs after impact) and simulated x-ray thereof for test 99-01. Figure 10-e is the actual radiograph from the 99-01 test showing the projectile in the 6-inch diagnostic gap upstream of Plate 6. As seen in Figure 10-f, the length of the residual projectile predicted by the hydrocode agrees with the 14 mm length measured on the test radiograph. Impact pressures calculated by CALE also indicate that HE (represented in this target by Plate 6) would be initiated with significant margin under these conditions. The computer runs also showed that the rod would penetrate as far as Plate 9, which was in good agreement with test results. Diameter of the crater in Plate 2 is about 3.5 cm which agrees well with test data.

Another verification of residual rod length was made for test 99-03, which used a target with surfaces at oblique incidence. Figure 11 shows selected frames from the 2-D CALE hydrocode simulation of test 99-03 including simulated x-rays and comparison to test data. The 13-mm residual rod length predicted residual rod length agrees well with the measurement from the test radiograph. CALE hydrocode results also show that HE would be initiated with significant margin under these conditions. This prediction was actually verified in tests 99-08 and 99-09, which used HE imbedded in the target.

2-D CALE hydrocode was also used to simulate HE burn. Figure 12 shows selected frames from simulation of tests 99-08 and 99-09. Propagation of the detonation wave and resulting deformation of target material are clearly seen. Predicted shock wave TOA were compared to test data and found in good agreement.

The 3-D CTH hydrocode was used to obtain higher fidelity simulations for tests involving oblique incidence (99-03 and subsequent). These studies were particularly useful to investigate the effects of oblique impact including the possibility of rod shatter and rod rotation. Figure 13 contains selected frames from simulations the rod impacting the tungsten alloy plate in Type 3 target. During the penetration process the rod erodes and is deformed. Total erosion is in agreement with previous data and simulations. The last frame shows an apparent counter-

clockwise rotation of the rod. This may provide an explanation for the seemingly asymmetric shape of the residual projectile seen in x-ray from tests 99-04, Figure 14.

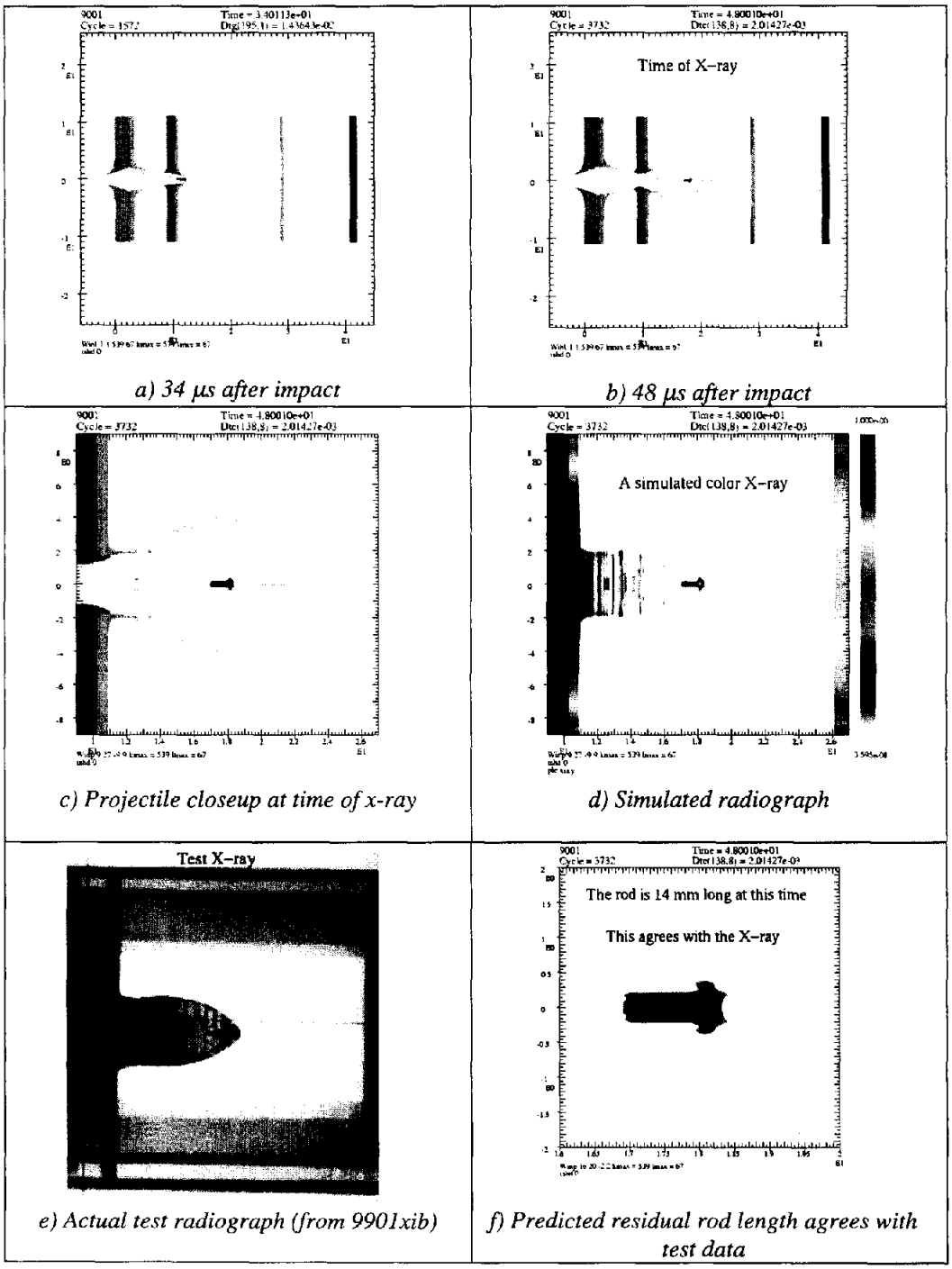

Figure 10. Comparison of residual rod length predicted by 2-D CALE to data from Test 99-01

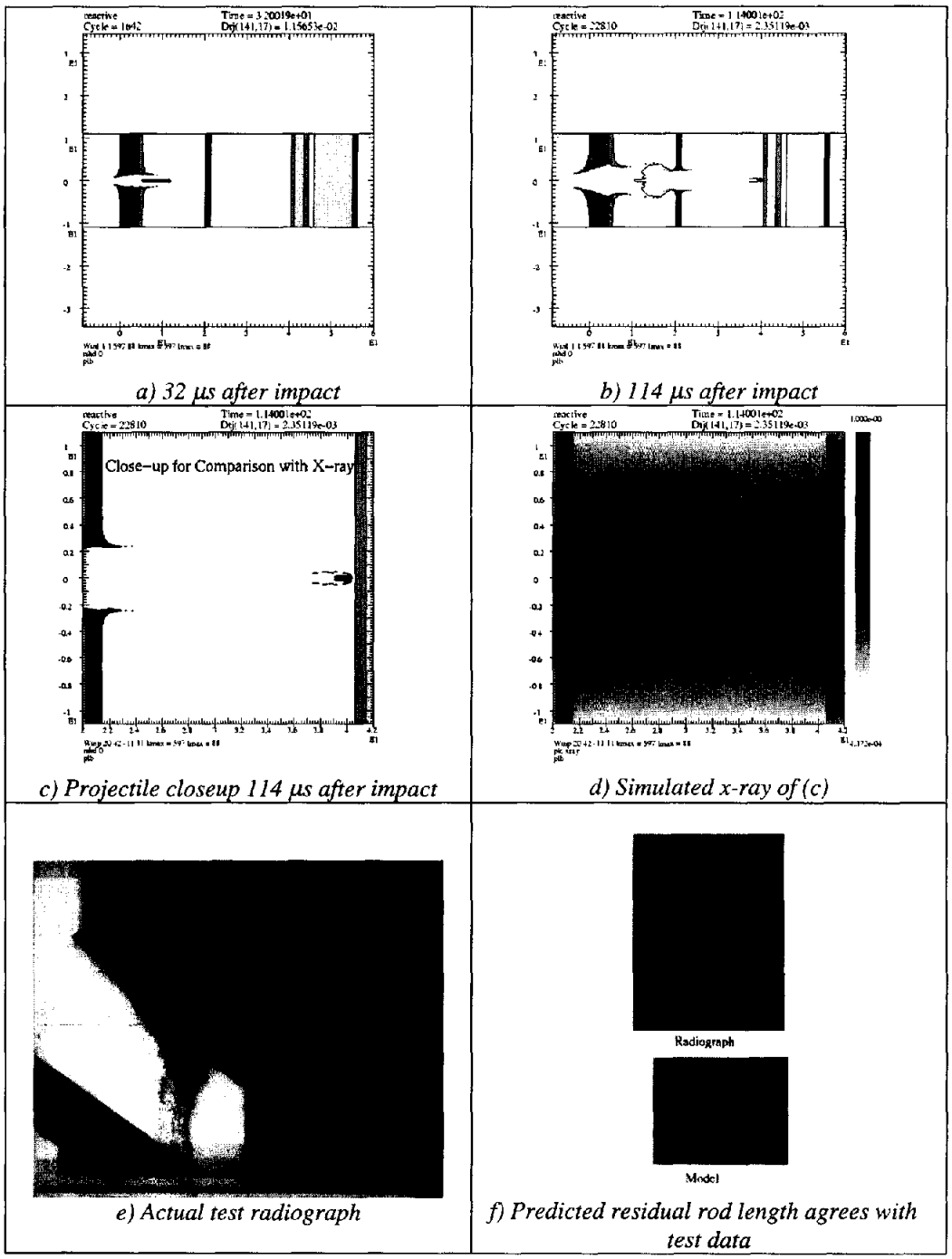

Figure 11. 2-D CALE simulation of Test 99-03 showing rod penetration into the target and analysis of residual rod length

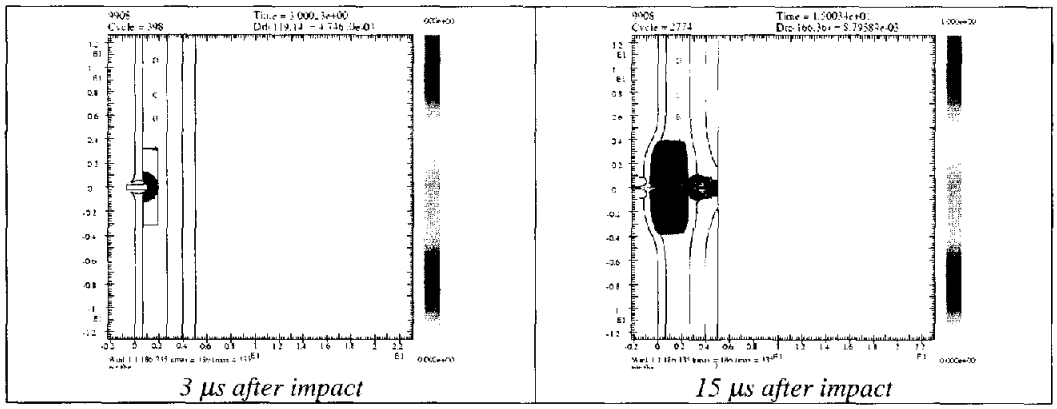

Figure 12. 2-D CALE simulation of Tests 99-08 and 9909 showing intiation of HE puck inside the target, propagation of detonation shock wave, and deformation of target material

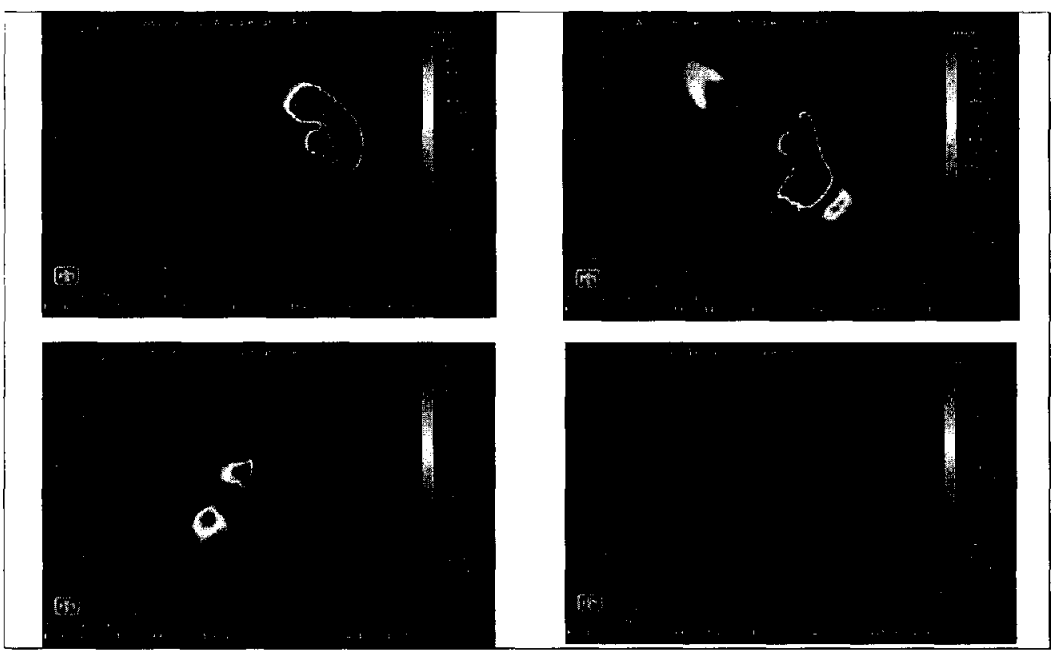

Figure 13. 3-D CTH simulation of Test 99-04 showing rod penetration of tungten plate at oblique angle of incidence and analysis of residual rod length

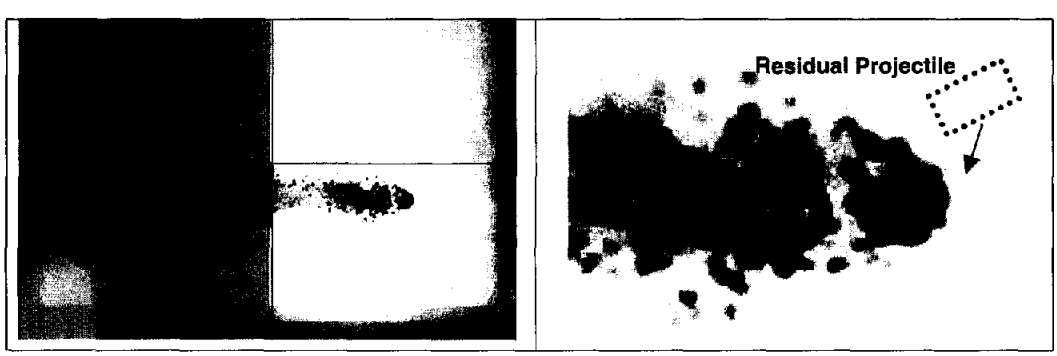

Figure 14. X-ray from Test 99-04 showing residual projectile (trailed by ejecta) with an apparent angle of attack (see closeup on the right)

CONCLUSION

This effort generated initial experimental data, which strongly confirms the KED lethality mechanism against uncertain targets. Test results verified rod erosion rates and rod penetration at oblique impact. In targets containing high explosive, the explosive was successfully initiated, thereby demonstrating that HEI criteria was exceeded. Excellent agreement between test data and hydrocode simulations indicates that hydrocodes can be used to investigate rod performance in velocity regimes not accessible on a ballistic range. Furthermore, test data provided an anchor for Boeing REAPER code, a fast running shotline processing evaluation tool. However, the work is far from complete because available data allows reliable predictions of KED lethality only in a very limited regime. A more extensive database should be generated to evaluate KED effectiveness in specific applications.

ACRONYMS

ARC	- Aerophysics Research Center	KV	- Kill vehicle
HE	- High explosive	LGG	- Light gas gun
HEI	- High explosive initiation	PSI	- Physical Sciences Incorporated
KED	- Kill enhancement device	TOA	- Time-of-arrival
HRE	- Huntington Research & Engineering	UAH	- University of Alabama in Hunstville

Acknowledgements —This project was conducted in the1998-99 period. Its success was made possible by a close collaboration of many individuals and several organizations. In particular, foundations for this work were established in the early 1990s by Don Stevenson of Rocketdyne working in with John Huntington of HRE and Peter Nebolsine of PSI. Dan Schwab and Peter Chu of Boeing provided a guidance in project planning. Resourcing the funds for this project became possible through persistent effort of Rees Padfield, Chief Engineer of Boeing Kinetic Energy Weapons, who also provided continuous inspiration and encouragement to the entire team. The experimental part of the project was carried out at the Aerophysics Research Center of the University of Alabama in Huntsville. Test planning and hydrocode simulation were performed by John Huntington and Steve Hancock of HRE, San Jose, CA. REAPER reanchoring and predictive test analyses were performed by Peter Nebolsine of PSI, Andover, MA.

REFERENCES

[1] J.A. Zukas, editor, *High Velocity Impact Dynamics*, John Willey & Sons, Inc., New York, NY, 1990
[2] C.E. Anderson, Jr., B.L. Morris, and D.L. Littlefield, A Penetration Mechanics Database, SwRI Report 3593/001, Southwest Research Institute, San Antonio, TX, 1992.
[3] J.R. Baker, "Rod Lethality Studies," NRL Report 6920, AFATL TR-69-1, Naval Research Laboratory, Washington, DC, July 1969.
[4] J.R. Baker and A. Williams, Hypervelocity penetration of plate targets by rod and rod-like projectiles, *Int. J. Impact Engng.*; **5**: 101-110, 1987
[5] P.E. Nebolsine, N.D. Humer, N.F. Harmon, and J.R. Baker, Statistical Analysis of NRL 1964-1969 Hypervelocity Rod-Plate Impact Data and Comparison to Recent Data, *Int. J. Impact Engng.1999*; **23**: 639-649
[6] V. Hohleer and A. Stilp, "Hypervelocity Impact of Rod Projectiles with L/D from 1 to 32," *Int. J. Impact Engng.* 1987; **5**: 323-331.
[7] P.E. Nebolsine, E.Y. Lo, and R.D. Ferguson, "Tungsten Pellet Fragment Field Characterization," *Int. J. Impact Engng.* 1995; **17**: 583-593.
[8] P.E. Nebolsine, E.Y. Lo, and R.D. Ferguson, "Simulation of Hypervelocity Impact Events at High Velocities," AIAA 94-4541, AIAA Space Programs and Technologies Conference, Huntsville, AL, 27-29 September 1994.
[9] P.E. Nebolsine and E.Y. Lo , "GBI KE Penetrator Alloy Selection Study, PSI report to Rocketdyne Division of Rockwell International (now Boeing), June 1996, document no. PSI-3067/TR-1446